ORIGINAL ARTICLE

The soil organic carbon stock and its influencing factors in a mountainous karst basin in P. R. China

Zhenming Zhang[1,2] · Yunchao Zhou[1,2,3] · Shijie Wang[3,4] · Xianfei Huang[1,2]

Abstract

Soil organic carbon represents a major carbon pool in terrestrial ecosystems. Currently, in karst areas, there is considerable uncertainty regarding the estimation of soil organic carbon pools due to limited profile numbers and heterogeneity. Using a grid-based sampling method, 2755 soil profiles consisting of 22,057 soil samples were analyzed to determine the spatial distribution and storage of soil organic carbon (SOC) in the Houzhai River Basin in the Guizhou Province in southwest China. The results suggest that the total SOC storages in the 0–20 and 0–100 cm soil horizons of the Houzhai River Basin are approximately 2.65×10^8 and 5.39×10^8 kg C, respectively. The differences in the soil bulk density between different soil types were considerable. The average soil bulk density of large mud field loam, which ranged from 1.25 to 1.52 g/cm^3, was significantly higher than that of the other soil types. The differences in soil organic carbon content were obvious as well. As soil depth increased, the organic carbon content gradually decreased. At a depth of 0–50 cm, the soil organic carbon content significantly decreased. In contrast, soil organic carbon content decreased slowly from 50 to 100 cm, indicating that a depth of 50 cm is the turning point for organic carbon content. The different degrees of soil organic carbon storage in different soil types were mainly caused by differences in organic carbon density. In karst regions, the soil parent material limits the spatial distribution of soil organic carbon, and soluble rock is the base development material. Soil thickness, slope gradient, and rock exposure are the primary factors leading to differences in SOC storage in different soil types. In addition, this study also suggests that increased attention should be paid to rock exposure in the assessment of SOC stocks in karst mountainous areas, such as the Houzhai River Basin.

Keywords Bare rock rate · Estimation method · Soil organic carbon storage · Small watershed · Karst

Introduction

Karst areas are unique ecosystems that differ from non-karst areas in terrain and landform, hydrothermal characteristics, and site-specific conditions that influence vegetation and soil development. Because of their special geological and climatic conditions, karst areas exhibit low environmental capacity, weak anti-interference, low stability, and poor self-regulation (Zheng et al. 2016; Chen et al. 2014; Zhou et al. 2010). In karst regions, the soil environment is coupled with bedrock outcrops and small soil stocks with a scattered and discontinuous distribution, and the micro-topography is complex and diverse, leading to the development of a discontinuous shallow soil of varying thickness. These factors complicate karst soil organic carbon density calculations (Ying et al. 2012). Due to the unique characteristics of the karst region, the method for estimating carbon density in non-karst areas is not suitable for these special areas. Many scholars have studied the karst ecosystem characteristics that influence soil organic carbon density heterogeneity. Currently, some indexes, such as the rate of rock coverage and soil thickness, have been considered in the estimation of SOC storage in karst areas (Koulouri

✉ Yunchao Zhou
yczhou@gzu.edu.cn

1   Forest Resource and Environment Research Center
    of Guizhou Province, Guizhou University, Guiyang 550025,
    China

2   College of Forestry, Guizhou University, Guiyang 550025,
    China

3   Puding Karst Ecosystem Research Station of Guizhou
    Province, Puding 562100, China

4   State Key Laboratory of Environmental Geochemistry,
    Institute of Geochemistry, Chinese Academy of Sciences,
    Guiyang 550002, China

and Giourga 2007; Schlesinger 1982), but other indexes have not. By investigating the spatial variability of related indexes, including soil distribution and acreage, rate of rock coverage, soil thickness, bulk density, and SOC content, in the plateau-type karst of small watersheds and revising the SOC density and storage relationship, a method of calculation based on soil type has been proposed to improve the reliability of SOC storage estimates for these areas. However, the publication of such research is rare.

Soil connects the atmosphere, hydrosphere, biosphere, and lithosphere. Soil carbon is an important part of the terrestrial carbon pool as well as an important basis for soil fertility (Weissert et al. 2016; Akpa et al. 2016; Bohn 1982). Soil carbon consists of organic carbon and inorganic carbon. The content of inorganic carbon is stable, exerting little influence on the carbon cycle (Fox and Bryan 1999; Kinsey-Henderson and Wilkinson 2013). Therefore, soil organic carbon (SOC) is the main factor affecting the carbon balance of terrestrial ecosystems (Pouyat et al. 2002). The transformation of SOC has a direct impact on the global carbon cycle, soil fertility and plant growth, and an indirect impact on terrestrial carbon stores, which makes SOC both an important indicator of soil quality and a comprehensive reflection of terrestrial productivity and environmental health (Niu et al. 2015). Serious human disturbance and fragility in karst ecosystems have caused severe land degradation with heavy losses of SOC that further decrease the sustainability of the ecosystem. Therefore, understanding the changes in the SOC of karst ecosystems not only contributes to an underlying theory for their ecological restoration and reconstruction but also becomes an important element for understanding the carbon cycle (Lal 2002).

The primary methods for calculating SOC include the soil-type method, life zone method, and model method (Pouyat et al. 2002). Due to the density of sampling points and sampling methods, both the geostatistical and life zone methods generate large errors, because they estimate the SOC of an entire study area based on a limited number of sampling points (Juan et al. 2013). However, the soil-type method, which is used more widely, employs a soil attribute database to estimate the SOC storage in a small or medium-sized area by summing all estimated SOC stocks for each soil type and its corresponding acreage (Grüneberg et al. 2013). Because the factors influencing SOC storage are poorly understood, the estimates by different people can be quite different, and it is difficult to determine, whose calculation is more accurate. Therefore, all factors that affect SOC content should be considered in the calculation.

The primary objective of this research was to perform a comprehensive analysis of the factors impacting the soil organic carbon in the Houzhai River Basin. Furthermore, we explored how the accuracy of the estimation methods varied with different soil types, soil depths, and SOC contents. This in-depth study of a karst area and the accurate estimation of its carbon pool provide a reference to inform regional sustainable development and the accurate estimation of the global soil carbon pool.

Materials and methods

Study region

The study region (105°40′43″–105°48′2″E, 26°12′29″–26°17′15″N) includes the towns of Chengguan, Maguan and Baiyan in Puding County of Guizhou Province, and it covers an area of 72 km². The elevation is between 1223.4 and 1567.4 m above sea level, and the air pressure is between 806.1 and 883.8 hpa. There are three major soil categories: limestone soil, paddy soil, and yellow soil. Vegetation includes cedarwood (*Cupressus funebris* Endl.), Chinese aspen (*Populus adenopoda* Maxim), Chinese mahogany [*Toona sinensis* (A. Juss.) Roem.], and Chinese pear [*Pyrus pyrifolia* (Burm.) Nakai.]. The main crops are paddy rice (*Oryza sativa* and *Oryza glaberrima*), corn (*Zea mays* Linn. Sp.), soybean [*Glycine max* (Linn.) Merr], and sunflower (*Helianthus annuus*).

Soil sampling

The study design followed a grid-based sampling method, and a total of 3180 sampling grids (150 m × 150 m) were established. Sampling sites were defined at the center of each sampling grid (Fig. 1). From March 2013 to January 2015, 2755 soil profiles consisting of 22,057 soil samples were determined according to designed sampling grids. Of the sampling sites, 425 were located, where sampling could not be performed, such as on a roadway or tractor road or in residential housing, industrial parks, or streams. Each profile was divided into 12 soil horizons (0–5, 5–10, 10–15, 15–20, 20–30, 30–40, 40–50, 50–60, 60–70, 70–80, 80–90, and 90–100 cm) if the soil thickness was equal to or greater than 95 cm. Otherwise, sampling was carried out to the actual soil depth. For instance, if a soil profile was 26 cm in depth, 5 soil samples were taken (0–5, 5–10, 10–15, 15–20, and 20–26 cm), and if a soil profile was 33 cm thick, 5 soil samples would also be taken (0–5, 5–10, 10–15, 15–20, and 20–30 cm).

Local information about each sampling point including the soil bulk density, soil thickness, rock coverage, and other indexes was measured and recorded at the time of sampling. Soil samples were air dried, ground, and prepared as required for laboratory analysis, and the SOC content was then tested and analyzed via the potassium dichromate method. Soil acreage was calculated using GIS technology and field surveys soil bulk density was measured layer by

Fig. 1 Location of Houzhai River Basin and the distribution of sample sites
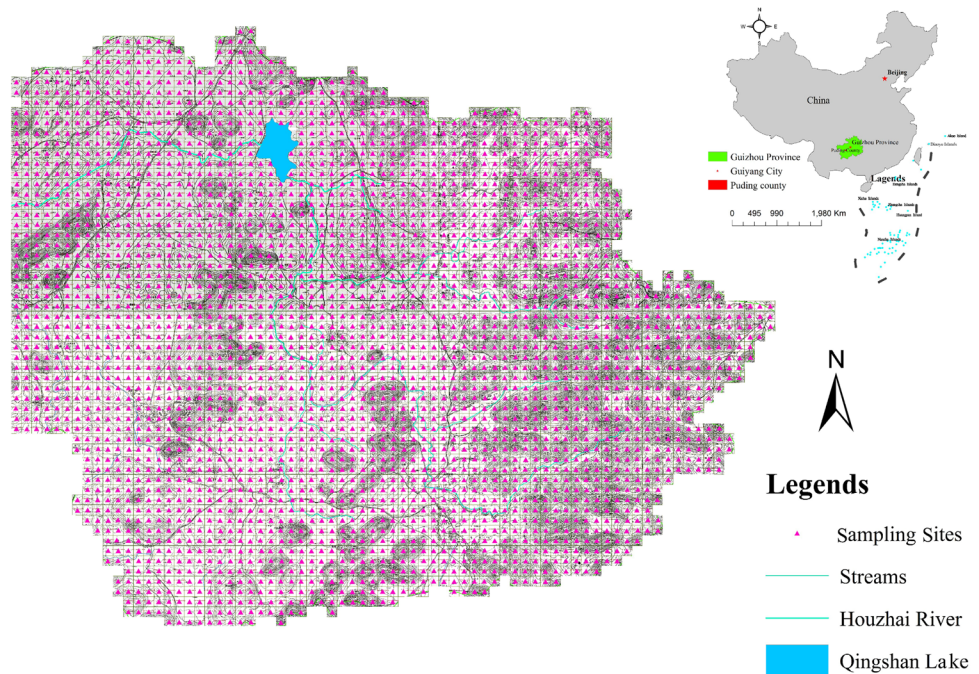
layer from the top to the bottom of the soil profile via the cutting-ring method (Nelson and Sommers 1982; Wang et al. 2010). Soil thickness was recorded in accordance with the type of ecological niche with a metal stick that was 60 or 120 cm long depending on the soil mass at different depths. Bare rock rate was surveyed using the line-transect method. Due to the complex karst landscape, this measurement would have been more accurate but less operable with a longer line transect. Therefore, the length of the transect was set at 10 m, and the grid cells with rock coverage were surveyed with a tape measure.

Soil bulk density (SBD) was determined at the time of sampling (cylindrical core method). For each layer of all soil profiles, 181.58 cm^3 of soil was sampled with a cutting ring ($r = 3.4$ cm, $h = 5$ cm), and the fresh weight was measured with a portable balance. Approximately 5 g of soil from each layer were collected into an aluminum cup, whose weight had been previously determined. Three milliliters of alcohol (95%) were added to the subsample and ignited (this was repeated three times), and the weight was determined pre- and post-calcination. The SBD was calculated using

$$\text{SBD} = \frac{(W_{\text{cr+s}} - W_{\text{cr}}) \times (W_{\text{post}} - W_{\text{cup}})}{(W_{\text{pre}} - W_{\text{cup}}) \times 181.58}, \tag{1}$$

where SBD is the soil bulk density (g/cm^3), W_{cr} is the weight of the cutting ring (g), $W_{\text{cr+s}}$ is the weight of the cutting ring with fresh soil (g), W_{cup} is the weight of the aluminum cup (g), W_{pre}, and W_{post} are the pre- and post-calcination weights of the aluminum cup with soil (g) and 181.58 is the volume of the cutting ring (cm^3).

Data analysis

Data from 2755 sampling points surveyed during the early stage of this program were analyzed. The soils could be divided into nine types on the basis of soil type as follows: 457 samples of yellow clay, 613 samples of rendzina, 397 samples of yellow limestone soil, 129 samples of large loam, 439 samples of small clay, 125 samples of white large loam, 106 samples of white sand, 185 samples of large mud field loam, and 304 samples of yellow clayey soil. Data analysis was conducted in Excel 2013 and ArcGIS 10.3 software.

Calculations and statistical analysis

To minimize the estimation error of the SOC stock, the error due to rock coverage in the karst area can be reduced by revising its bare rock rate (Zhang et al. 2017):

$$\text{SOCD}_{i,j} = C_{\text{soc}_{i,j}} \times \rho_{i,j} \times T_{i,j} \times 10^{-2} \tag{2}$$

where $\text{SOCD}_{i,j}$ is the SOC density in the ith layer of soil type j (kg/m^2), $C_{\text{soc}_{i,j}}$ is the SOC content in the ith layer of soil type j (g/kg), $\rho_{i,j}$ is the soil bulk density of the ith layer of soil type j (g/cm^3), $T_{i,j}$ is the soil thickness of the ith layer of soil type j (cm), and 10^{-2} is the conversion coefficient:

$$\text{SOCS} = \sum_{j=1}^{m} \sum_{i=1}^{n} \text{SOCD}_{i,j} \times S_j \times (1 - \delta_j) \times (1 - G_j) \times 10^3, \tag{3}$$

where SOCS is the total stock of SOC in the study area (kg C), S_j is the soil acreage of soil type j (km^2), 10^3 is the unit conversion factor, δ_j is the bare rock rate in the sampling area of soil type j (%), and G_j is the fraction of the gravel volume that is greater than 2 mm in soil type j. The other indexes are the same, as in Eq. (2).

Results

Soil thickness and rock exposure in the study region

As mentioned above, 425 of the sampling sites were designated in places, where sampling could not be performed. One was situated on a railway, 120 on roadways, 10 on tractor roads, 36 in streams, 124 in residential housing, 100 in industrial parks, and 34 in factories.

Detailed information on the soil thickness and rock exposure of the Houzhai River Basin is listed in Tables 1 and 2, and spatial information related to these factors is shown in Fig. 2. First, it is obvious that the thicknesses of soils on mountains are generally lower than those of soils in flat areas or on small hills, and rock exposure in mountainous areas is much greater than that in flat areas.

Second, the mean soil thickness and rock exposure values varied significantly with the different soil types.

The limestone soil, paddy soil, and yellow soil are interwoven throughout the study area, so the soils in this watershed are highly heterogeneous. The limestone soil areas suffered from severe stony desertification and are scattered with rock exposure. With rock coverage being considered, soil coverage in the area is overestimated. Therefore, the soil acreage value should be revised by considering rock acreage. In addition, the rate of rock coverage is very different in different soil types. The mean rock coverage rate in the rendzina area was approximately 43.34%, which is the highest value, while it was 29.22%, the lowest value, in the large loam of tilled soil. There was little rock exposure in the three major tillage areas as well as the yellow clay, large mud field loam, and yellow clayey soils, so the rate of rock acreage in these areas is very low.

Soil bulk densities and SOC concentrations of different soil types in the study area

Soil bulk density is of great importance in the assessment of SOC contents. As shown in Table 3, the differences in soil bulk densities among the different soil types were large.

**Table 1** Statistics of soil thickness a of different soil types in study region

Soil type	N	Minimum (cm)	Maximum (cm)	Mean (cm)	Standard deviation	Variance	Skewness	Kurtosis
RD	613	5.00	100.00	61.73	32.83	53.18	− 0.072	− 1.58
YL	397	7.00	100.00	37.47	25.55	68.19	0.90	− 0.13
YC	457	7.00	100.00	85.50	24.12	28.21	− 1.74	1.92
YCL	304	19.00	100.00	86.98	22.58	25.96	− 1.51	0.79
LU	185	13.00	100.00	80.13	27.99	34.93	− 1.04	− 0.44
LL	129	9.00	100.00	73.52	29.56	40.21	− 0.57	− 1.22
WL	125	11.00	100.00	50.87	30.01	58.99	1.10	− 0.98
SC	439	7.00	100.00	57.02	30.08	52.75	0.26	− 1.34
WS	106	6.00	100.00	36.21	27.98	77.27	1.33	0.60

RD rendzina, *YL* yellow lime soil, *YC* yellow clay, *YCL* yellow clayey soil, *LU* large mud field loam, *LL* large loam, *WL* white large loam, *SC* small clay, *WS* white sand

Table 2 Statistics of rock exposure of different soil types in study region

Soil type	N	Minimum (cm)	Maximum (cm)	Mean (cm)	Standard deviation	Variance	Skewness	Kurtosis
RD	613	0.00	0.95	0.30	0.25	83.33	0.42	− 0.97
YL	397	0.00	0.92	0.25	0.23	92	0.79	− 0.19
YC	457	0.00	0.91	0.06	0.16	266.67	2.79	6.89
YCL	304	0.00	0.73	0.13	0.10	76.92	5.48	30.46
LU	185	0.00	0.70	0.03	0.11	366.67	3.95	15.57
LL	129	0.00	0.82	0.10	0.18	180	1.88	2.73
WL	125	0.00	0.90	0.18	0.21	116.67	1.33	1.16
SC	439	0.00	0.90	0.15	0.19	126.67	1.29	1.07
WS	106	0.00	0.91	0.20	0.22	110	0.99	0.46

Fig. 2 Spatial information of soils thickness and rock exposure in the study region
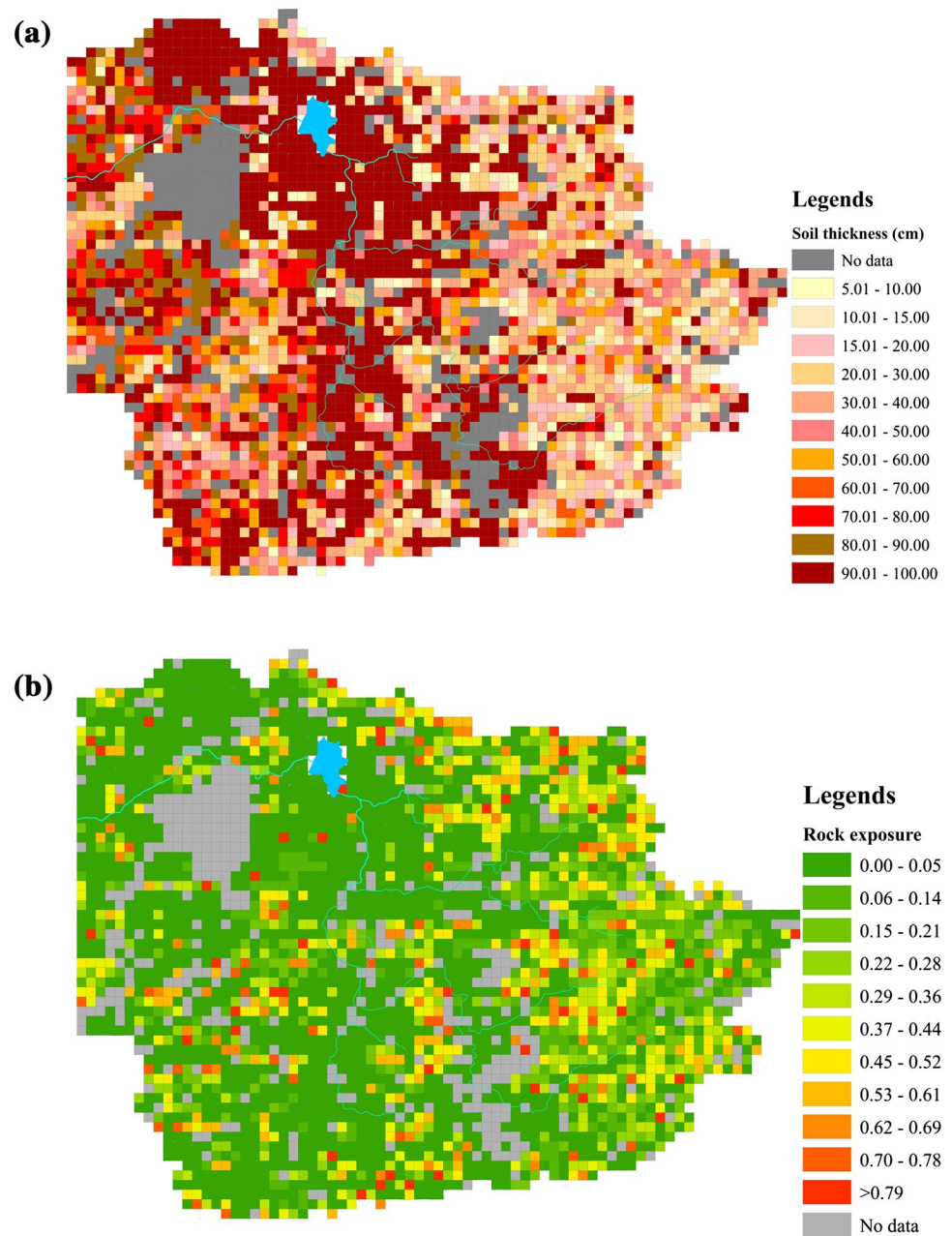
The average soil bulk density of large mud field loam, which ranged from 1.25 to 1.52 g/cm³, was significantly higher than that of other soil types. Among the different soil layers, the soil bulk density of rendzina gradually increased with soil depth, while that of large loam and large mud field loam first increased and then tended to stabilize. In contrast, the soil bulk density of yellow clay, yellow clayey soil, yellow lime soil, small clay, white sand, and white large loam first increased and then decreased as soil depth increased. The largest soil bulk density values of rendzina and large loam occurred at the bottom of the profile, while the largest values for the remaining soil types were observed in the transition zone between the A and B layers.

The average SOC concentrations of different soil types are shown in Fig. 3. Vertically, the distribution of the SOC content in the profile was the most obvious characteristic. With increasing soil depth, the organic carbon content gradually decreased. In the 0–50-cm soil horizon, the content of SOC decreased significantly, but at depths greater than 50 cm, SOC content decreased slowly. This finding suggests that 50 cm is the turning point in the graph of the SOC profile. The discrepancies in the average SOC contents of the different soil types mainly existed in the top 50 cm of the soil layer. There were no significant differences among the average SOC contents of the different soil types in the 50–100-cm soil layer. The SOC content of the

Table 3 Profile characteristics of soil bulk density of different soil types (g cm^{-3})

Soil type	0–10 cm	10–20 cm	20–30 cm	30–40 cm	40–50 cm	50–60 cm	60–70 cm	70–80 cm	80–90 cm	90–100 cm
RD	1.15(0.017)A	1.20(0.037)A	1.30(0.037)A	1.37(0.018)BC	1.38(0.007)B	1.39(0.029)AB	1.40(0.054)B	1.44(0.054)B	1.46(0.029)BA	1.44(0.077)B
YL	1.20(0.020)A	1.25(0.036)A	1.29(0.057)A	1.35(0.033)A	1.37(0.028)AB	1.38(0.008)A	1.40(0.010)B	1.39(0.010)B	1.35(0.049)AB	1.32(0.009)A
YC	1.21(0.009)D	1.28(0.041)A	1.33(0.009)A	1.32(0.017)D	1.33(0.092)A	1.32(0.034)A	1.32(0.029)A	1.31(0.021)CD	1.29(0.057)A	1.28(0.030)A
YCL	1.29(0.023)BC	1.37(0.020)B	1.49(0.059)B	1.45(0.029)BA	1.43(0.020)AB	1.43(0.054)B	1.41(0.054)B	1.39(0.022)B	1.39(0.020)B	1.35(0.033)AB
LU	1.25(0.019)B	1.36(0.028)AB	1.52(0.029)BA	1.46(0.025)B	1.48(0.059)B	1.47(0.059)B	1.45(0.059)B	1.42(0.054)B	1.42(0.054)B	1.43(0.027)B
LL	1.27(0.035)A	1.36(0.018)BC	1.43(0.059)B	1.42(0.010)B	1.43(0.025)B	1.45(0.020)AB	1.44(0.027)B	1.42(0.054)B	1.44(0.077)B	1.44(0.026)A
WL	1.19(0.016)CD	1.26(0.021)A	1.34(0.018)DE	1.35(0.033)AB	1.37(0.019)B	1.36(0.028)AB	1.39(0.007)B	1.38(0.022)B	1.36(0.049)AB	1.26[a]
SC	1.26(0.020)DE	1.34(0.037)AB	1.40(0.018)B	1.39(0.015)B	1.39(0.007)B	1.41(0.054)B	1.38(0.028)AB	1.37(0.019)B	1.38(0.028)AB	1.37(0.020) B
WS	1.27(0.020)E	1.29(0.043)AB	1.39(0.015)B	1.42(0.054)B	1.40(0.007)B	1.43(0.025)B	1.43(0.010)B	1.42(0.054)B	1.38(0.029)AB	1.32(0.052)AB

Means and standard errors. Within columns, values followed by the same capital letter (A–E) are not significantly different ($p < 0.05$) in between one soil horizon in different land uses ([a]$n = 1$, no standard error values)

surface soil (0–10 cm) was the highest for all soil types, and it was ranked as follows: rendzina > yellow lime soil > white sand > large mud field loam > white large loam > small clay > yellow clayey soil > large loam > yellow clay. However, the distribution of the SOC concentration throughout the profile of the different soil types (0–100-cm soil horizon) conforms to a different model.

Soil organic carbon density in the Houzhai River Basin

In the present study, the SOC density at the 0–20 cm and 0–100 cm soil thickness horizons were calculated for each designated sampling grid, and this spatial information for the study region is presented in Fig. 4. Obviously, SOC density exhibits high inhomogeneity in response to soil thickness and rock exposure. In the Houzhai River Basin, the SOC density for the 0–20 cm and the 0–100 cm soil horizons ranged from 0.09 to 19.54 kg/m^2 and from 0.09 to 44.66 kg/m^2 with mean values of 4.28 and 8.70 kg/m^2, respectively. Detailed information about the SOC density of different soil types is listed in Table 4. The mean SOC density values of the 0 to 20-cm soil horizon of the different soil types descended in the following sequence: large mud field loam > yellow clayey soil > rendzina > large loam > yellow lime soil > small clay > white sand > white large loam > yellow clay. Conversely, the mean SOC density values of the 0–100-cm soil horizon of the different soil types descended in the following sequence: white large loam > large loam > large mud field loam > small clay > yellow clay > yellow lime soil > yellow clayey soil > white sand > rendzina. The SOC density of the 10-cm-thick soil layer gradually decreased as soil depth increased before gradually stabilizing in the deeper soil horizon. The mean SOC density for the 0–100-cm soil horizon in the Houzhai River Basin was approximately 8.70 kg/m^2, but the average density of soil organic carbon in China at 100 cm is 10.53 kg/m^2. Due to the large spatial variation in soil thickness, the 10-cm thick karst SOC density and the mean SOC density for China were compared. The average SOC density in the top 10 cm of the soil in the Houzhai River Basin was 2.09 kg/m^2, but the average 10-cm SOC density in China is 1.21 kg/m^2. The SOC density in the upper 10 cm of the soils in the study region is approximately 1.7 times the mean for China.

Soil organic carbon storage in the Houzhai River Basin

The total SOC storage in the 0–100-cm soil horizon of the Houzhai River Basin was approximately 5.39 × 10^8 kg, and the SOC content in each sampling grid is shown in

Fig. 3 Profile characteristics of soil organic carbon of different soil types in study area
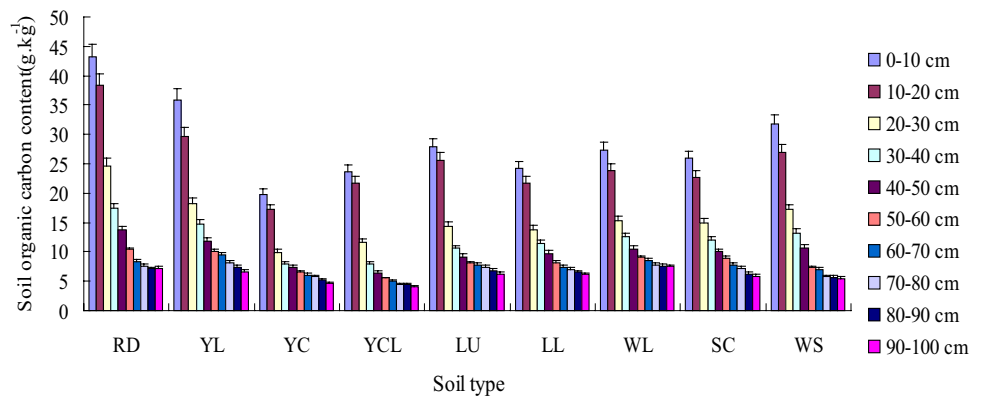

Fig. 4 Spatial information of SOC density in study region (**a** for 0–20 cm soil horizon, **b** for, 0–100 soil horizon) (unit: kg/m^2)
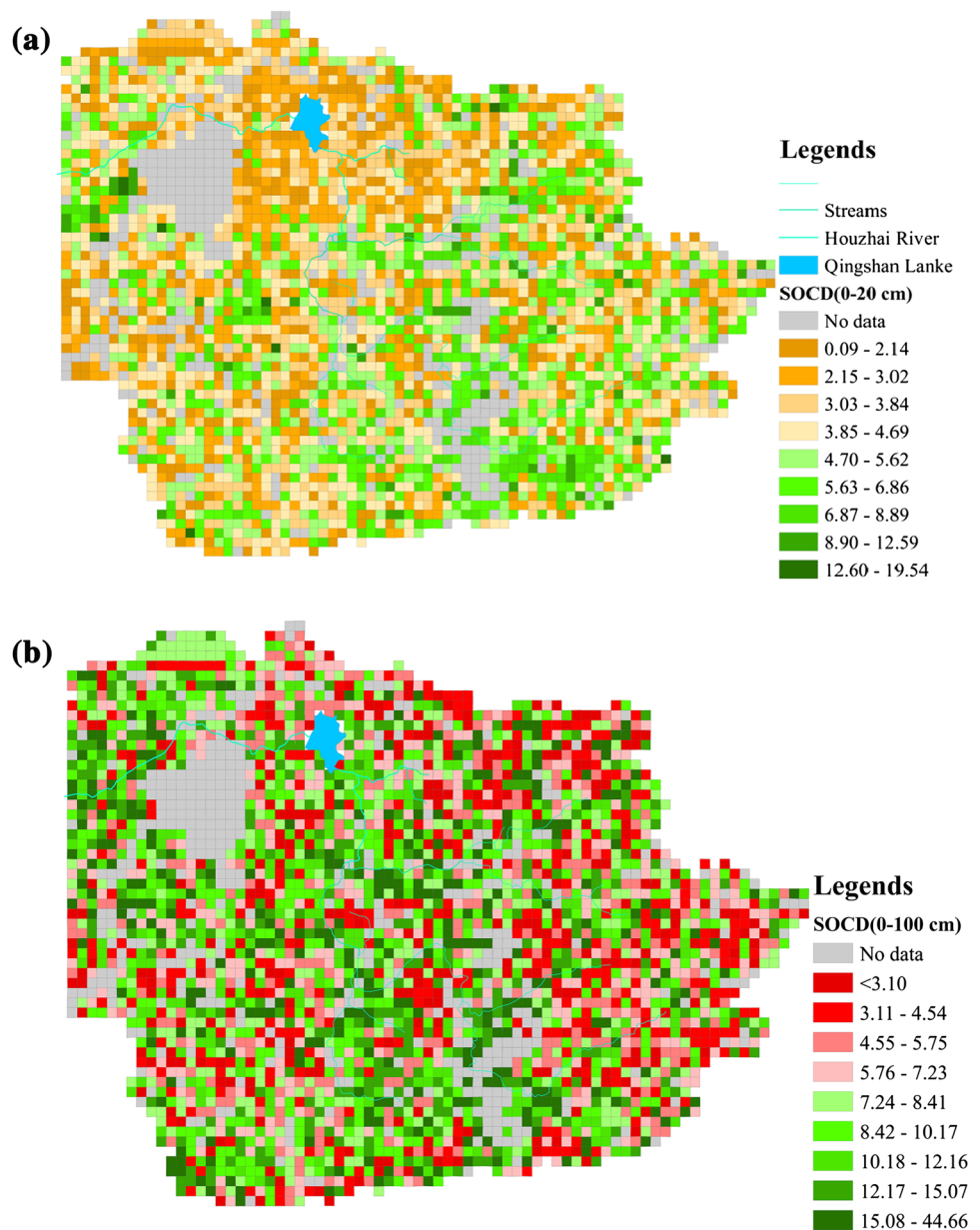
Table 4 Statistics of SOC density of different Soil types

Soil type	N	20 cm				100 cm			
		Range	Mean	Standard deviation	CV	Range	Mean	Standard deviation	CV
RD	613	0.22–29.54	4.46	2.81	63.00	0.29–35.23	6.29	5.01	79.65
YL	397	0.43–16.14	4.33	2.07	47.81	0.51–31.13	7.56	4.69	62.04
YC	457	0.08–9.40	3.31	1.41	42.60	0.09–33.84	8.68	4.69	54.03
YCL	304	0.66–10.16	5.01	1.82	36.33	1.29–26.65	10.82	4.31	39.83
LU	185	1.71–11.57	5.61	1.76	31.37	2.26–44.66	13.19	6.02	45.64
LL	129	0.96–10.08	4.35	1.65	37.93	1.53–29.93	10.38	5.27	50.77
WL	125	0.57–10.11	3.96	1.86	46.97	0.92–29.92	7.91	5.82	73.58
SC	439	0.42–10.54	4.11	1.65	40.15	0.58–24.78	8.34	3.34	40.05
WS	106	0.09–10.42	4.09	2.01	49.14	0.09–20.19	6.27	4.32	68.90

Fig. 5. The SOC for the different grids ranged from 2112 to 1,004,938 kg. The stored SOC in the 0–10-, 0–20-, and 0–30-cm soil horizons of the Houzhai River Basin were 1.48×10^8, 2.65×10^8, and 3.44×10^8 kg, respectively.

The differences in the stored SOC among soil types were mainly caused by the differences in the SOC density of the different soil types. As shown in Fig. 6, the SOC storage in topsoil (0–20 cm) of the different soil types was ranked as follows: large mud field loam > yellow clayey soil > large loam > white large loam > rendzina > yellow lime soil > small clay > white sand > yellow clay (Fig. 6a). The SOC storage of the whole profile (0–100 cm) was ranked as follows: large mud field loam > white large loam > yellow clayey soil > large loam > rendzina > small clay > yellow clay > yellow
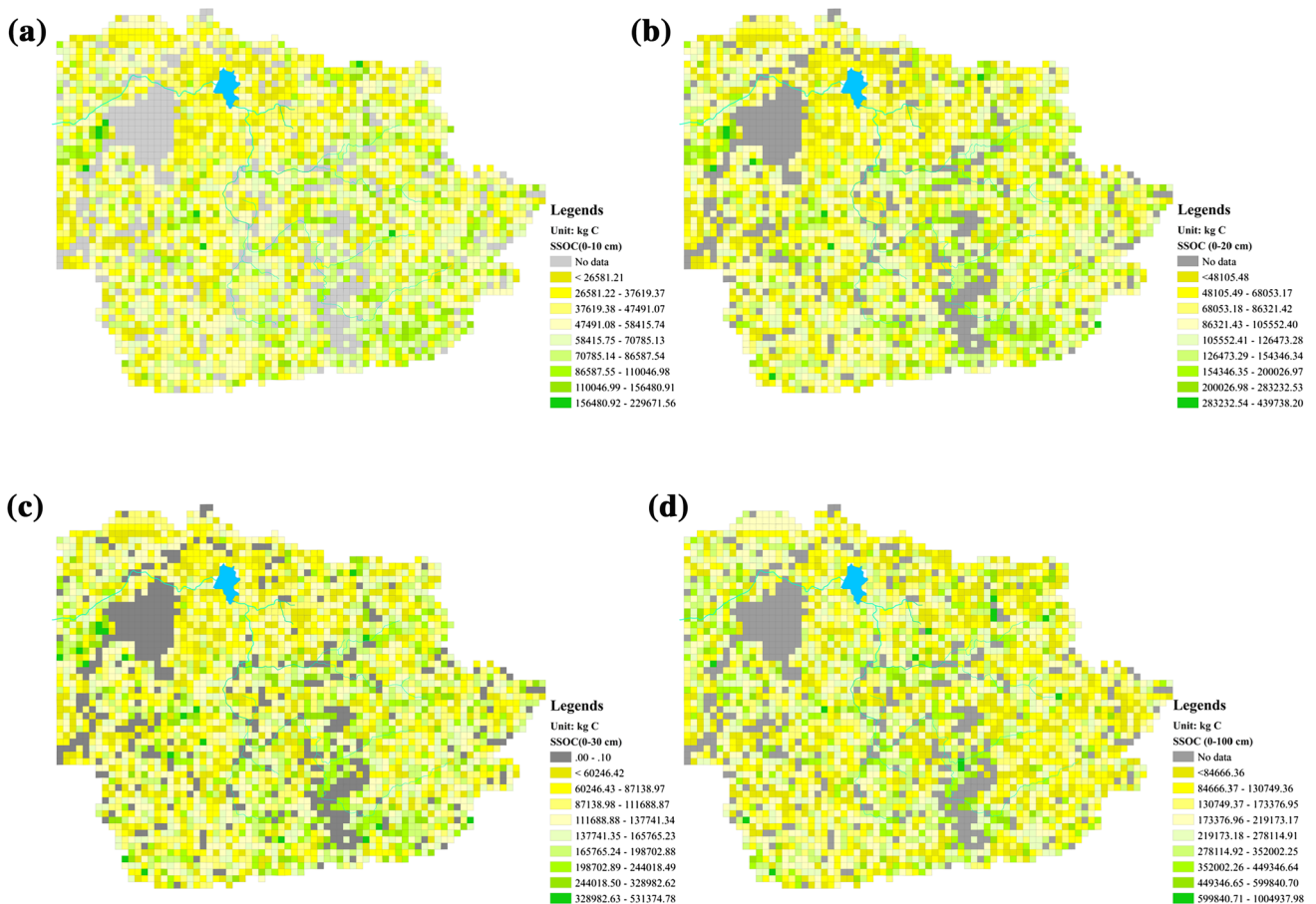

(a)

Legends
Unit: kg C
SSOC(0-10 cm)
No data
< 26581.21
26581.22 - 37619.37
37619.38 - 47491.07
47491.08 - 58415.74
58415.75 - 70785.13
70785.14 - 86587.54
86587.55 - 110046.98
110046.99 - 156480.91
156480.92 - 229671.56

(b)

Legends
Unit: kg C
SSOC (0-20 cm)
No data
<48105.48
48105.49 - 68053.17
68053.18 - 86321.42
86321.43 - 105552.40
105552.41 - 126473.28
126473.29 - 154346.34
154346.35 - 200026.97
200026.98 - 283232.53
283232.54 - 439738.20

(c)

Legends
Unit: kg C
SSOC(0-30 cm)
.00 - .10
< 60246.42
60246.43 - 87138.97
87138.98 - 111688.87
111688.88 - 137741.34
137741.35 - 165765.23
165765.24 - 198702.88
198702.89 - 244018.49
244018.50 - 328982.62
328982.63 - 531374.78

(d)

Legends
Unit: kg C
SSOC (0-100 cm)
No data
<84666.36
84666.37 - 130749.36
130749.37 - 173376.95
173376.96 - 219173.17
219173.18 - 278114.91
278114.92 - 352002.25
352002.26 - 449346.64
449346.65 - 599840.70
599840.71 - 1004937.98

Fig. 5 Spatial information of SSOC stores in each designed grid in Houzhai River Basin

Fig. 6 Percentage of SSOC in different Soil types in Houzhai River Basin (**a** for 0–20 cm soil horizon, **b** for 0–100 cm soil horizon)

(a)

10.31% 6.40% 10.66%
13.71% 10.12%
12.32% 10.21%
13.84% 12.43%

- ▦ rendzina
- ▦ yellow lime soil
- ▦ yellow clay
- ▦ yellow clayey soil
- ▦ large mud field loam
- ▦ large loam
- ▦ white large loam
- ▦ small clay
- ▦ white sand

(b)

9.82% 9.37% 10.86%
12.14% 10.67%
12.19% 8.17%
14.30% 12.48%

- ▦ rendzina
- ▦ yellow lime soil
- ▦ yellow clay
- ▦ yellow clayey soil
- ▦ large mud field loam
- ▦ large loam
- ▦ white large loam
- ▦ small clay
- ▦ white sand
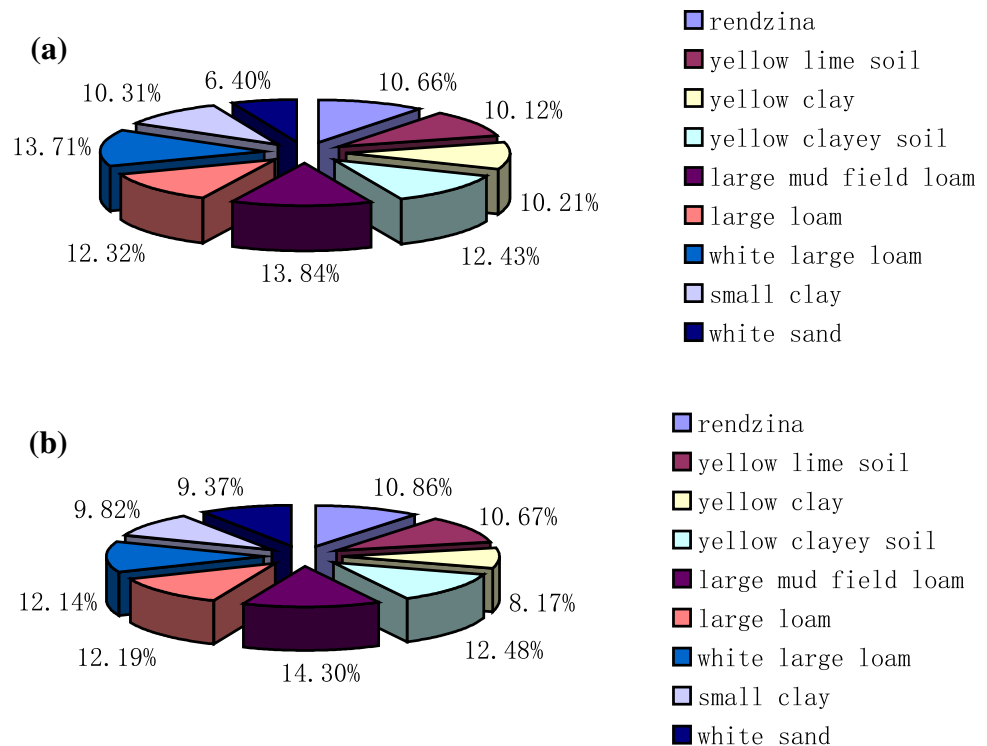
lime soil > white sand (Fig. 6b). At the same time, the soil-forming environment and the soil-forming characteristics of the different soil types were different. During the field surveys, most of the large mud field loam was flooded, and the soil layer under the water and wet vegetation was in a state of gas reduction for a long time. This state is conducive to the accumulation of organic matter but not its decomposition. Therefore, the SOC density of the large mud field loam was very high, and the SOC storage was also relatively large. Most of the white sand and yellow clay were distributed in steeply sloping areas, and the corresponding vegetation coverage was very low. Species of small shrubs and bushes were the dominant vegetation, and the decay of plant residues was slow, while the mineralization of organic matter was fast. We believe that this is the main reason why the organic carbon accumulation speed in these soils was very weak.

Discussion

The study region is part of a karst landform and is characterized by high topographical diversity and soil nutrient spatial in homogeneity. The factors affecting SOC concentration and storage in this region are extremely complex. Therefore, SOC concentration and density in this region are highly spatially variable.

Comparison of organic carbon content in karst and non-karst areas

The content and dynamic equilibrium of soil organic carbon are vital to the assessment of soil quality and soil health, and they directly affect soil fertility and crop production. Some studies indicate that soil organic carbon has great influence on soil structure formation and stability, water maintenance, bioavailability of plant nutrients, soil buffering properties, and soil biodiversity (Adak et al. 2014). Therefore, it plays an important role in the mitigation and regulation of a series of soil processes related to soil degradation and soil productivity. The results of the present study suggest that the soil organic carbon contents in the top soil layers (0–20 cm) in the Houzhai River Basin range from 1.61 to 119.11 g/kg with a mean value of 25.07 g/kg. In comparison with the previous studies, the mean value is obviously lower than the soil organic carbon contents in the non-karst area (Parrasalcántara et al. 2015), which likely indicates that the soil in the karst area is infertile and thus the weakness of the karst ecological system (Wu et al. 2015).

The total amount of soil and soil organic carbon in the karst area was very low. The soil organic carbon density in the upper soil layers (0–20 cm) of the sloping karst lands was approximately 4.28 kg m^{-2}, which was significantly lower than that in non-karst areas. The unique karst geological environment has a profound influence on soil organic carbon density that results in bare rock, soil erosion, discontinuous soil cover, habitat complexity, and widely exposed bedrock, and a large number of weathering residues accumulate in

the rock fractures and funnels. Plant root development with discontinuous shallow soils scatters the distribution of soils. The thickness of the karst soil varies greatly with most of the soil being only 4–9 cm deep. Therefore, the total amount of soil in the karst area is significantly lower than in non-karst areas. In addition, the decline of the fragile karst ecosystem is a complex process in which human disturbance is a strong driving force, vegetation reduction is an important incentive, land productivity degradation is an innate character, and increasing desertification landscapes are a symbol.

Effects of different soil and soil rock types on SOC concentrations

Some research has shown that the soil parent material has a remarkable impact on the spatial distribution of SOC (Fang et al. 2015). In karst regions, soluble rock was the base development material, and the insoluble residue from the corrosion of carbonate rock was the main source of the soil (Fu et al. 2014). The tropical peak cluster and needle karst landforms were largely developed under humid and rainy climate conditions, leading to the wide distribution of limestone soil throughout the peak forest plain or the arc peak plain (Xu et al. 2013). Therefore, the rock types in the study area were varied, and the spatial distribution patterns of the soils were different. In the studied basin, the rock types are mainly dolomite, limestone, marl, sand–shale, and quaternary yellow clay (Gong et al. 2012). The dolomite and limestone were mainly distributed in the peak upper reaches and the peak cluster depression area, and their distribution area was very large.

However, the distribution area of the dolomite and limestone in the karst and butte areas was relatively low. The peak, peak cluster, and regional soil thicknesses were relatively shallow, but the amount of soil in the depression region was profound. The sandstone area was marl that was primarily distributed in the upstream slope land and paddy fields, whose distribution area was small (Fontaine et al. 2007). Other regions also had a small number of areas with sporadically distributed soil that was relatively shallow. The quaternary yellow clay was mainly distributed in the middle and lower reaches of the hillock; their distribution area was large, and the amount of soil was profound. Based on the results of the analysis, the impact of soil type and lithology on the spatial variation in SOC was remarkable. The soil types reflected differences of soil-forming conditions and soil-forming processes. Because the soil-forming conditions and soil-forming processes of the three types of soil in the study area (lime soil, paddy soil, and yellow soil) were obviously different, significant differences in soil organic carbon storage resulted (Table 5).

Effect of slope gradient and slope position on the SOC stock of the study region

Based on geologic records, the soil slope position was divided into the bottom, the lower part, the upper middle part, the upper part, and the top part of the mountains in the Houzhai River Basin. As shown in Table 6, rocks were exposed along the slope positions, affecting the soil depth, the SOC contents, and the SOC density. The soil depth was closely

Table 5 Lithologic distribution characteristics of the Houzhai River Basin

Rock type	Space distribution	Geomorphic type	Soil type
Dolomite	Upstream concentration distribution, zonal distribution in the middle and lower reaches	Peak cluster, laeuna	Calcareous soil, paddy soil
Limestone	Upstream concentration distribution, zonal distribution in the lower reaches	Peak cluster, laeuna	Calcareous soil, paddy soil
Marlite	Upstream block distribution	Peak cluster, laeuna	Calcareous soil
Sand–shale stone	Upstream block distribution	Laeuna	Yellow soil, paddy soil
Quaternary yellow clay	Concentration area distribution in the middle and lower reaches	Downland	Yellow soil, paddy soil

Table 6 Effect of slope position on rock exposure, soil thickness, SBD, SOC concentration, and SOC density

	Slope aspect		Slope position				
	Shady aspect	Sunny aspect	BM	LPM	CPM	UPM	TPM
Rock exposure (%)	0.26	0.19	0.16	0.22	0.27	0.27	0.27
Soil thickness (cm)	63.57	47.12	61.82	50.23	43.25	35.73	49.72
COC Concentration (0–10 cm) (g kg^{-1})	34.33	29.85	22.41	28.37	34.03	32.23	25.11
SOC density (0–10 cm) (kg m^{-2})	2.87	3.89	1.96	1.68	2.08	2.16	2.11

BM bottom of mountains, *LPM* lower part of mountains, *CPM* central part of mountains, *UPM* upper part of mountains, *TPM* top part of mountains

related to the slope position, and declined from 61.81 to 35.73 cm. The rate of exposed rock gradually increased from 16 to 27% and then stabilized. The density of SOC (0–10 cm) increased from 1.96 to 2.16 kg/m^2 and then declined to 2.11 kg/m^2. Because of the influence of soil depth, rock contents and SOC from the bottom of the slope to the top part of the mountains. The most of central part, the upper part, and the top part of the mountains were woodland and shrub land that were rich in organic matter and characterized by vegetation in good condition. In addition, the higher terrain and reduced human influence resulted in a higher SOC content. In contrast, most of the bottom part of the slope and the lower mountains were agricultural land, which was poor in vegetation and soil input. The SOC content was low in this area. In general, the sunny aspect was dry, so the SOC decomposed faster, and its content was lower. The content of SOC was higher on the shady aspect; thus, the content and density of SOC were higher than on the sunny aspect.

Effects of other environmental factors on the SOC stock of the study region

The correlation analyses between the SOC density and the environmental factors in the Houzhai River Basin is shown in Table 7. The density of SOC exhibited a remarkable correlation with elevation, soil depth, gravel content, slope gradient, and rate of exposed rock ($p < 0.01$). However, multiple environmental factors were correlated with each other, so the contribution of each environmental factor on density of SOC could not be determined. Therefore, a principal component analysis (PCA) was needed to extract the major factors influencing the density of SOC. Slope position, elevation, slope gradient, and slope aspect were regarded as the main indicators of the first principal component, which consisted of the main topographic parameters driving SOC in the Houzhai River Basin. The soil bulk density, soil type, rock content, and soil depth were regarded as the main indicators of the second principal component, which was treated as a factor that correlated with soil formation. The vegetation was regarded as the main indicator of the third principal component, which was considered the vegetation factor. To reveal the contribution of each environmental factor to SOC density, a stepwise regression analysis (SR) was used to select the principal component index, which included the gravel content, elevation, slope position, soil depth, slope gradient and the rate of exposed rock, and the following multiple linear regression equation describing the relationship between SOC density (dependent variable) and each environmental factor (independent variables) was established:

$$SOCD = 1.86D + 8.21L + 0.15A + 3.654B - 1089.946 \ (R^2 = 0.54, p < 0.001),$$

Table 7 Correlation between the density of SOC and different environmental factors

Environmental factor	Elevation	Soil depth	Content of rock	Slope gradient	Slope position	Slope direction	Unit weight	Parent material	Rate of exposed rock	SOC density (0–20 cm)	SOC density (0–100 cm)
Elevation	1										
Soil depth	−0.320[a]	1									
Content of rock	0.210[a]	−0.14[b]	1								
Slope gradient	−0.09	0.23	−0.48	1							
Slope position					1						
Slope direction				0.41	0.20	1					
Unit weight	0.62[b]	0.54[b]	0.42[a]	0.42	0.31	0.65	1				
Parent materials	0.21	−0.16	0.76[a]	0.49[b]	0.73	−0.17	0.68	1			
Rate of exposed rock	0.21[a]	−0.33[a]	0.53[a]	0.30	0.75[b]	−0.46	0.71	0.91[a]	1		
SOC density (0–20 cm)	0.42[a]	0.12[b]	−0.61[a]	−0.42[a]	0.78	0.33	0.65[b]	0.21[b]	−0.731[a]	1	
SOC density (0–100 cm)	0.17[a]	0.48[a]	−0.21[a]	−0.54[a]	0.29	0.46	0.73[b]	0.27[b]	−0.21[a]	0.86[a]	1

[a] Correlation is significant at the 0.01 level

[b] Correlation is significant at the 0.05 level

where SOCD is the SOC density (kg m^{-2}), D is the soil depth, L is the rate of exposed rock (%), A is the elevation (m), and B is the gravel content (%). Soil depth was most closely correlated with SOC density ($\beta = 0.67$) followed by the rate of exposed rock ($\beta = 0.23$), the gravel content ($\beta = 0.15$) and elevation ($\beta = 0.11$). Overall, SOC density was comprehensively affected by different environmental factors in the Houzhai River Basin.

Conclusion

Using a grid-based sampling method, 2755 soil profiles consisting of 22,057 soil samples were sampled and analyzed. We believe that the SOC density in the 0–20- and 0–100-cm soil horizons in the Houzhai River Basin in the Guizhou Province of southwest China ranged from 0.09 to 19.54 kg C m^{-2} and 0.09 to 44.66 kg/m^2 with mean values of 4.28 and 8.70 kg/m^2, respectively. The SOC stored in the 0–20 and 0–100 cm soil horizons of the Houzhai River Basin was 2.65×10^8 and 5.39×10^8 kg, respectively.

In the Houzhai River Basin, soil type is a critical factor that is closely associated with soil bulk density and SOC concentration. In addition, the correlation analyses of SOC density and different environmental factors in the Houzhai River Basin were inconclusive. Therefore, principal component analysis (PCA) was needed to extract the primary factors influencing the density of SOC. The slope position, elevation, slope gradient and slope aspect, which were main factors of SOC in the Houzhai River Basin, were determined to be the main indicators of the first principal component and were treated as topographic parameters. The soil bulk density, soil type, gravel content, and soil depth were regarded as the main indicators of the second principal component and were treated as soil formation correlation factors. Human activities and geographic characteristics are believed to be the primary factors that lead to high in homogeneity of SOC in mountainous karst areas.

References

Adak T, Singha A, Kumar K, Shukla SK, Singh A, Singhkumar V (2014) Soil organic carbon, dehydrogenase activity, nutrient availability and leaf nutrient content as affected by organic and inorganic source of nutrient in mango orchard soil. J Soil Sci Plant Nutr 14:394–406

Akpa SIC, Odeh IOA, Bishop TFA, Hartemink AE, Amapu IY (2016) Total soil organic carbon and carbon sequestration potential in Nigeria. Geoderma 271:202–215

Bohn HL (1982) Estimate of organic carbon in world soils. Soil Sci Soc Am J 46:1118–1119

Chen XB, Zheng H, Zhang W, He XY, Li L, Wu JS, Huang DY, Su YR (2014) Effects of land cover on soil organic carbon stock in a karst landscape with discontinuous soil distribution. J Mt Sci 11:774–781

Fang F, Hu YK, Gong YM, Tang HP (2015) Soil organic carbon of different decomposition rate and its relation to microbial activity in saline-alkali desert ecosystem. Pol J Ecol 63:102–109

Fontaine S, Barot S, Barre P (2007) Stability of organic carbon in deep soil layers controlled by fresh carbon supply. Nature 450:277–280

Fox DM, Bryan RB (1999) The relationship of soil loss by in terrill erosion to slope gradient. CATENA 38:211–222

Fu G, Zhang XZ, Zhou YT, Yu CQ, Shen ZX (2014) Partitioning sources of ecosystem and soil respiration in an alpine meadow of Tibet Plateau using regression method. Pol J Ecol 62:17–24

Gong YM, Hu YK, Fang F, Liu YY, Li KH, Zhang GM (2012) Carbon storage and vertical distribution in three shrubland communities in Gurbantunggut Desert, Uygur Autonomous Region of Xinjiang, Northwest China. Chin Geogra 22:541–549

Grüneberg E, Schning I, Hessenmller D, Schulze ED, Weisser WW (2013) Organic layer and clay content control soil organic carbon stocks in density fractions of differently managed German beech forests. Forest Ecol Manag 303:1–10

Juan A, Roque O, Noelia GF, Antonio RN, Maria A, Javier GP, Maria MM (2013) Land use and climate change impacts on soil organic carbon stocks in semi-arid Spain. J Soils Sedim 13:265–277

Kinsey-Henderson AE, Wilkinson SN (2013) Evaluating Shuttle radar and interpolated DEMs for slope gradient and soil erosion estimation in low relief terrain. Environ Modell Softw 40:128–139

Koulouri M, Giourga C (2007) Land abandonment and slope gradient as key factors of soil erosion in Mediterranean terraced lands. CATENA 69:274–281

Lal R (2002) Soil carbon sequestration in china through agricultural intensification and restoration of degraded and desertified ecosystems. Land Degrad Dev 13:469–478

Nelson DW, Sommers LE (1982) Total carbon, organic carbon, and organic matter. In: Page AL, Miller RH, Keeney DR (eds) Methods of soil analysis, agronomy, part 2, 2nd edn. ASA and SSSA, Madison, pp 539–577

Niu X, Gao P, Li Y, Li X (2015) Impact of different afforestation systems on soil organic carbon distribution characteristics of limestone mountains. Pol J Environ Stud 24:2543–2552

Parrasalcántara L, Lozanogarcía B, Brevik EC, Cerdà A (2015) Soil organic carbon stocks assessment in Mediterranean natural areas: a comparison of entire soil profiles and soil control sections. J Environ Manag 155:219–228

Pouyat RV, Groffman PM, Yesilonis ID, Hernandez L (2002) Soil carbon pools and fluxes in urban ecosystems. Environ Pollut 116:107–118

Schlesinger WH (1982) Carbon storage in the caliche of arid soils a case study from arizona. Soil Sci 133:247–255

Wang YG, Li Y, Ye XH, Chu Y, Wang XP (2010) Profile storage of organic/inorganic carbon in soil: from forest to desert. Sci Total Environ 408:1925–1931. https://doi.org/10.1016/j.scitotenv.2010.01.015

Weissert LF, Salmond JA, Schwendenmann L (2016) Variability of soil organic carbon stocks and soil CO$_2$ efflux across urban land use and soil cover types. Geoderma 271:80–90

Wu M, Liu SJ, Ye YY, Zhang W, Wang KL, Chen HS (2015) Spatial heterogeneity and storage assessment method of surface soil

organic carbon in high bulk-rock ratio slopes of Karst Regions. Chin J Eco Agric 6:676–685 **(in Chinese with English abstract)**

Xu XF, Thornton PE, Post WM (2013) A global analysis of soil microbial biomass carbon, nitrogen and phosphorus in terrestrial ecosystems. Glob Ecol Biogeogr 22:737–749

Ying B, Xiao SZ, Xiong KN, Cheng QW, Luo JS (2012) Comparative studies of the distribution characteristics of rocky desertification and land use/land cover classes in typical areas of Guizhou province, China. Environ Earth Sci 71:631–645

Zhang ZM, Zhou YC, Wang SJ, Huang XF (2017) Estimation of soil organic carbon storage and its fractions in a small karst watershed. Acta Geochim 1:1–12

Zheng T, Wu XQ, Dai EF, Zhao D (2016) SOC storage and potential of grasslands from 2000 to 2012 in central and eastern Inner Mongolia, China. J Arid Land 8:364–374

Zhou YC, Wang SJ, Lu HM, Xie L, Xiao D (2010) Forest soil heterogeneity and soil sampling protocols on limestone outctops: example from SW China. Acta Carsol 39:115–122